Chemistry Research Journal, 2020, 5(1):16-31

Available online www.chemrj.org

Research Article

ISSN: 2455-8990
CODEN(USA): CRJHA5

A Quantum-chemical study of the relationships between electronic structure and affinities for the serotonin transporter protein and the 5-HT$_{1A}$ receptor in a series of 2H-pyrido[1,2-c]pyrimidine derivatives

Juan S. Gómez-Jeria*, Nicolás González-Ponce

Quantum Pharmacology Unit, Department of Chemistry, Faculty of Sciences, University of Chile. Las Palmeras 3425, Ñuñoa, Santiago 7800003, Chile
J.S. Gómez-Jeria: facien03@uchile.cl

Abstract Some 2H-pyrido[1,2-c]pyrimidine derivatives present affinity for the 5-HT$_{1A}$ receptor and the serotonin transporter protein. In this paper we present the results of the search of relationships between the electronic structure of these molecules and the abovementioned affinities. The Klopman-Peradejordi-Gómez method was employed. Statistically significant equations were obtained for both affinities. Starting from the QSAR results we built the 2D-pharemacophores including the possible interactions with the binding site(s).

Keywords QSAR, common skeleton, DFT, electronic structure, pharmacophore, KPG model, 5-HT$_{1A}$ receptor, serotonin transporter protein, 2H-pyrido[1,2-c]pyrimidine

Introduction

Serotonin (5-hydroxytryptamine or 5-HT) is a neurotransmitter that modulates neural activity and a varied range of neuropsychological processes. The 5-HT receptors are found in the central and peripheral nervous systems. They can be divided into 7 families (5-HT$_1$, ..., 5-HT$_7$). All families are G protein-coupled receptors with the exception of the 5-HT$_3$ family which is a ligand-gated ion channel.

The 5-HT$_{1A}$ receptor is a subtype belonging to the 5-HT$_1$ family and is the most widespread of all the serotonin receptors [1-7]. Its activation induces the secretion of many hormones including adrenocorticotropic hormone, β-endorphin, cortisol, corticosterone, growth hormone oxytocin and prolactin.

The serotonin transporter (SERT) is a protein that transports serotonin from the synaptic cleft back to the presynaptic neuron [8]. It is the target of many antidepressant medications of the selective serotonin reuptake inhibitors and tricyclic antidepressant classes. Many groups of molecules binding to the serotonin receptors and the SERT protein have been synthesized [6, 9-22].

We have been studying for a longtime the relationships between electronic structure and affinity for the various serotonin receptors for a diversity of molecular systems [23-38].

Recently the synthesis of a group of 2H-pyrido[1,2-c]pyrimidine derivatives presenting affinity for the 5-HT$_{1A}$ receptors and the serotonin transporter protein was reported [39].As another contribution to the knowledge of the mode of binding of these new compounds we present here the results of a study of the relationships between their electronic structure and their affinity for the abovementioned structures, SERT and 5-HT$_{1A}$ receptor.

Methods, models and calculations

The molecules and receptor binding affinities are presented in Fig. 1 and Table 1 [39].

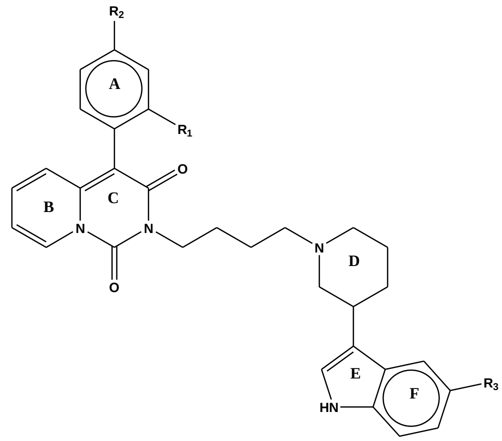

Figure 1: General formula of molecules

Table 1: 2H-pyrido[1,2-c]pyrimidine derivatives.

Molecule	R_1	R_2	R_3	$log_{10}(K_i)$ ($5\text{-}HT_{1A}$)	$log_{10}(K_i)$ (SERT)
1	H	H	H	1.34	1.83
2	Cl	H	H	1.70	2.01
3	F	H	H	1.72	2.38
4	CH_3	H	H	2.01	1.88
5	OCH_3	H	H	2.12	2.61
6	H	Cl	H	2.47	1.91
7	H	F	H	1.66	1.66
8	H	CH_3	H	1.80	2.32
9	H	OCH_3	H	1.62	1.61
10	H	H	F	2.32	0.90
11	Cl	H	F	2.58	2.41
12	F	H	F	2.34	2.06
13	CH_3	H	F	2.58	2.53
14	OCH_3	H	F	1.90	2.07
15	H	Cl	F	2.19	1.93
16	H	F	F	2.17	1.48
17	H	CH_3	F	2.13	2.13
18	H	OCH_3	F	2.15	1.43
19	H	H	OCH_3	2.42	2.39
20	Cl	H	OCH_3	2.25	2.66
21	F	H	OCH_3	2.11	3.22
22	CH_3	H	OCH_3	2.68	1.94
23	OCH_3	H	OCH_3	1.84	2.59
24	H	Cl	OCH_3	2.41	2.69
25	H	F	OCH_3	2.45	2.28
26	H	CH_3	OCH_3	2.52	2.24
27	H	OCH_3	OCH_3	1.79	1.93

Models and methods

The tool employed here is the Klopman-Peradejordi-Gómez (KPG) method. As the method has been fully reviewed recently we refer the reader to the literature [41-52]. We shall discuss only the results obtained here. Originally, the KPG method is a formal linear relationship between the drug-site affinity constant and a set of local atomic reactivity indices derived from the statistical-mechanical definition of the equilibrium constant. To them the socalled orientational parameters of the substituent were added. Recently it was shown that, under definite circumstances, this linear relationship could be extended to any biological activity. Finally, a new set of local atomic reactivity indices was generated within the Hartree-Fock framework and integrated into the model. The success of the KPG method is unquestionable [23, 53-62].

Calculations [40]

The electronic structure of all molecules was calculated within the Density Functional Theory (DFT) at the B3LYP/6-31G(d,p) level with full geometry optimization. The Gaussian suite of programs was used [63]. The information needed to calculate the numerical values for the LARIs was obtained from the Gaussian results with the D-Cent-QSAR software [64]. All the electron populations smaller than or equal to 0.01 e were considered as zero. Negative electron populations coming from Mulliken Population Analysis were corrected as usual [65]. As the resolution of the system of linear equations is not possible because we have not experimental data, we employed Linear Multiple Regression Analysis (LMRA) techniques to find the best solution. For each case, a matrix containing the dependent variable (log(K_i) in this case) and the local atomic reactivity indices of all atoms of the common skeleton as independent variables was built. The Statistica software was used for LMRA [66]. The common skeleton numbering is shown in Fig. 2.

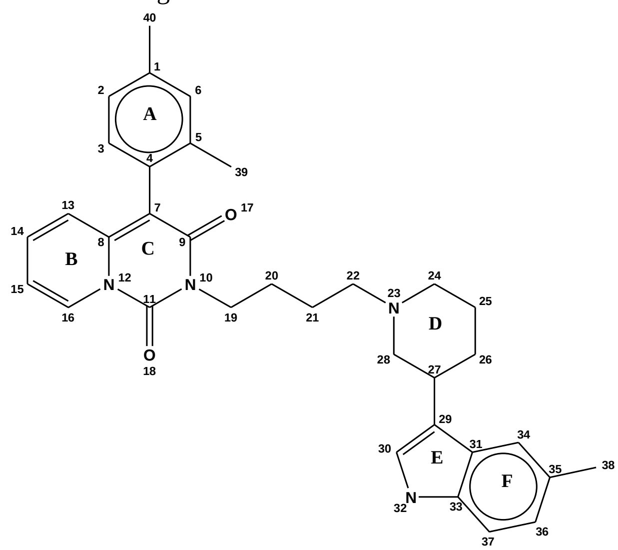

Figure 2: Common skeleton numbering

Atoms 38, 39 and 40 correspond to the atoms of the substituents that are directly attached to the rings.

Results

Results for 5-HT$_{1A}$ receptor affinity.

The best statistically significant equation is:

$$\log(K_i) = 2.45 + 0.29S_{33}^{E}(HOMO-2)^{*} - 0.70S_{40}^{N}(LUMO+2)^{*} + \\ +0.004S_{6}^{N}(LUMO+1)^{*} + 0.85S_{19}^{N}(LUMO)^{*} \quad (1)$$

with n=23, R=0.95, R^2=0.91, adj-R^2=0.88, F(4,18)=43.14 (p<0.000001) and SD=0.11. No outliers were detected and no residuals fall outside the ±2σ limits. Here, S_{33}^{E}(HOMO-2)* is the electrophilic superdelocalizability of the third highest occupied MO localized on atom 33, S_{40}^{N}(LUMO+2)* is the nucleophilic superdelocalizability of the third lowest empty MO localized on atom 40, S_{6}^{N}(LUMO+1)* is the nucleophilic superdelocalizability of the second lowest empty MO localized on atom 6 and S_{19}^{N}(LUMO)* is the nucleophilic superdelocalizability of the lowest empty MO localized on atom 19.Tables 2 and 3 show the beta coefficients, the results of the t-test for significance of coefficients and the matrix of squared correlation coefficients for the variables of Eq. 1. There are no significant internal correlations between independent variables (Table 3). Figure 3 displays the plot of observed *vs.* calculated $\log(K_i)$.

Table 2: Beta coefficients and t-test for significance of coefficients in Eq. 1

	Beta	t(18)	p-level
S_{33}^{E}(HOMO-2)*	0.78	10.60	0.000000
S_{40}^{N}(LUMO+2)*	-0.57	-6.98	0.000002
S_{6}^{N}(LUMO+1)*	0.40	4.80	0.0001
S_{19}^{N}(LUMO)*	0.25	3.27	0.004

Table 3: Matrix of squared correlation coefficients for the variables in Eq. 1

	S_{33}^{E}(HOMO-2)*	S_{40}^{N}(LUMO+2)*	S_{6}^{N}(LUMO+1)*
S_{33}^{E}(HOMO-2)*	1.00		
S_{40}^{N}(LUMO+2)*	0.00	1.00	
S_{6}^{N}(LUMO+1)*	0.02	0.17	1.00
S_{19}^{N}(LUMO)*	0.03	0.00	0.06

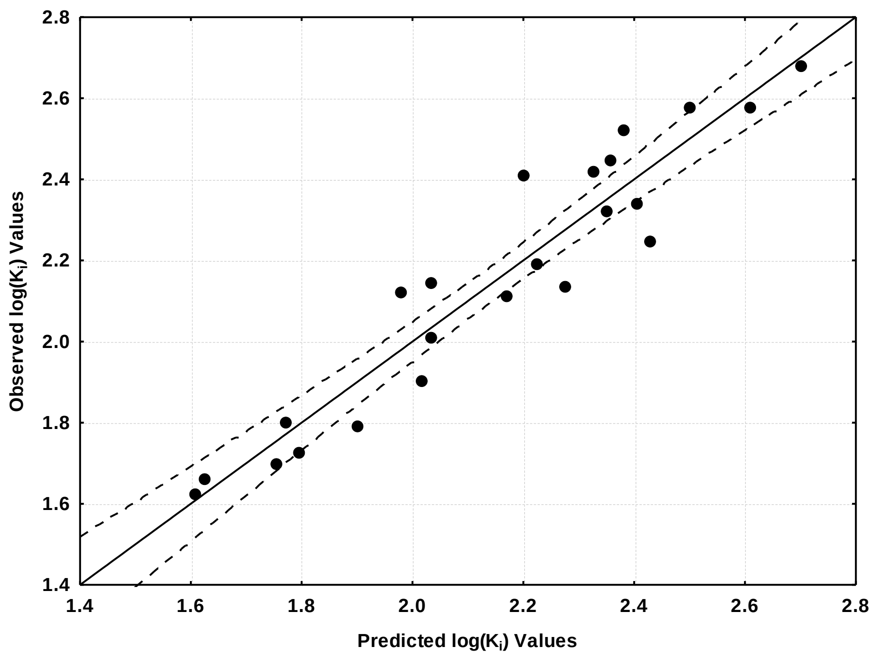

Figure 3: Plot of predicted vs. observed $\log(K_i)$ values (Eq. 1). Dashed lines denote the 95% confidence interval

The associated statistical parameters of Eq. 1 indicate that this equation is statistically significant and that the variation of the numerical values of a group of four local atomic reactivity indices of atoms of the common skeleton explains about 88% of the variation of $\log(K_i)$. Figure 3, spanning about 1.2 orders of magnitude, shows that there is a good correlation of observed *versus* calculated values.

Results for serotonin transporter protein (SERT) affinity

The best statistically significant equation is

$$\log(K_i) = -4.44 + 1.83S_{13}^{E}(HOMO-1)^* - 0.77S_{37}^{E}(HOMO)^* + 4.93S_{21}^{N}(LUMO+1)^* + \\ +2.64S_{26}^{N}(LUMO+2)^* - 1.29\mu_{10} - 2.23F_{10}(LUMO+1)^* - 0.73S_{24}^{N}(LUMO)^* + \\ +1.43F_{15}(HOMO-1)^* \quad (2)$$

with n=26, R=0.97, R^2=0.93, adj-R^2=0.90, F(8,17)=29.82 (p<0.000001) and SD=0.13. No outliers were detected and no residuals fall outside the ±2σ limits. Here, S_{13}^{E}(HOMO-1)* is the electrophilic superdelocalizability of the second highest occupied MO localized on atom 13, S_{37}^{E}(HOMO)* is the electrophilic superdelocalizability of the highest occupied MO localized on atom 37, S_{21}^{N}(LUMO+1)* is the nucleophilic superdelocalizability of the second lowest empty MO localized on atom 21, S_{26}^{N}(LUMO+2)* is the nucleophilic superdelocalizability of the third lowest empty MO localized on atom 26, μ_{10} is the local atomic electronic chemical potential, F_{10}(LUMO+1)* is the Fukui index of the second lowest empty MO localized on atom 10, S_{24}^{N}(LUMO)* is the nucleophilic superdelocalizability of the lowest empty MO localized on atom 24 and F_{15}(HOMO-2)* is the Fukui index of the third highest occupied MO localized on atom 15.Tables 4 and 5 show the beta coefficients, the results of the t-test for significance of coefficients and the matrix of squared correlation coefficients for the variables of Eq. 2. There are no significant internal correlations between independent variables (Table 5). Figure 4 displays the plot of observed *vs.* calculated log(K_i).

Table 4: Beta coefficients and t-test for significance of coefficients in Eq. 2

Variable	Beta	t(17)	p-level
S_{13}^{E}(HOMO-1)*	0.51	6.57	0.000005
S_{37}^{E}(HOMO)*	-0.34	-4.00	0.0009
S_{21}^{N}(LUMO+1)*	0.47	6.18	0.00001
S_{26}^{N}(LUMO+2)*	0.54	6.84	0.000003
μ_{10}	-0.30	-3.56	0.002
F_{10}(LUMO+1)*	-0.24	-3.64	0.002
S_{24}^{N}(LUMO)*	-0.24	-2.94	0.009
F_{15}(HOMO-2)*	0.20	2.18	0.04

Table 5: Matrix of squared correlation coefficients for the variables in Eq. 2

	S_{37}^{E}(HOMO)*	S_{37}^{E}(HOMO)*	S_{21}^{N}(LUMO+1)*	S_{26}^{N}(LUMO+2)*	μ_{10}	F_{10}(LUMO+1)*	S_{24}^{N}(LUMO)*
S_{37}^{E}(HOMO)*	0.00	1.00					
S_{21}^{N}(LUMO+1)*	0.07	0.01	1.00				
S_{26}^{N}(LUMO+2)*	0.01	0.02	0.00	1.00			
μ_{10}	0.01	0.02	0.18	0.02	1.00		
F_{10}(LUMO+1)*	0.00	0.00	0.01	0.01	0.02	1.00	
S_{24}^{N}(LUMO)*	0.00	0.25	0.00	0.10	0.03	0.04	1.00
F_{15}(HOMO-2)*	0.09	0.18	0.01	0.20	0.06	0.00	0.08

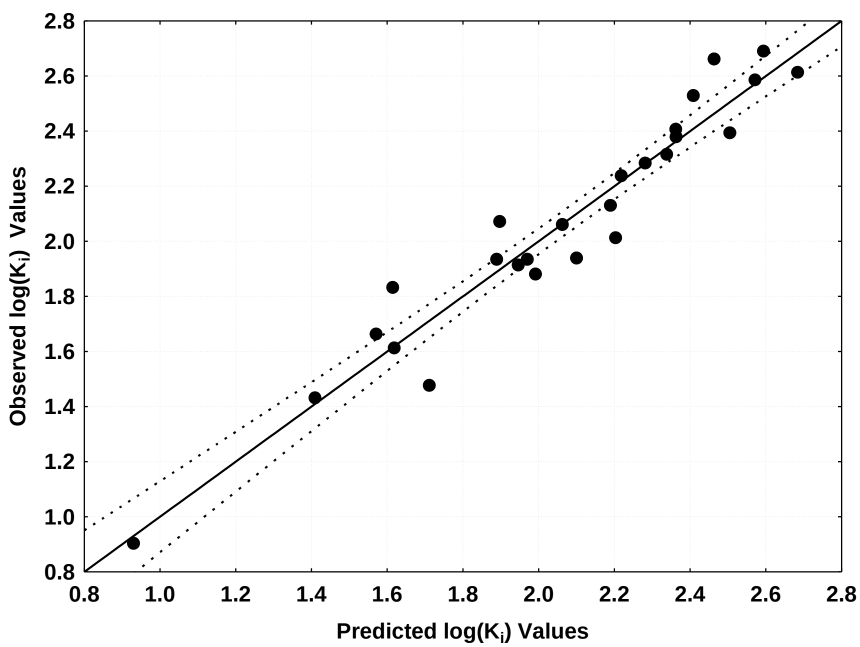

Figure 4: Plot of predicted vs. observed log(K_i) values (Eq. 2). Dashed lines denote the 95% confidence interval

The associated statistical parameters of Eq. 2 indicate that this equation is statistically significant and that the variation of the numerical values of a group of eight local atomic reactivity indices of atoms of the common skeleton explains about 90% of the variation of log(K_i).Figure 4, spanning about 2 orders of magnitude, shows that there is a good correlation of observed *versus* calculated values.

Local Molecular Orbitals

When a local atomic reactivity index of an inner occupied MO (i.e., HOMO-1 and/or HOMO-2) or of a higher empty MO (LUMO+1 and/or LUMO+2) appears in one equation, it indicates that the remaining of the upper occupied MOs (for example, if HOMO-2 appears, upper means HOMO-1 and HOMO) or the remaining of the empty MOs (for example, if LUMO+1 appears, lower means the LUMO) also contribute to the interaction. Their absence in the equation means only that the variation of their numerical values is not statistically significant. Tables 6 to 8 show the local molecular orbitals of all atoms appearing in Eq. 1 and 2.

Table 6: Local molecular orbitals of atoms 6, 10, 12 and 15

Mol.	Atom 6	Atom 10	Atom 13	Atom 15
1 (131)	125π126π127π-133π134π136π	125σ126π127σ-132π137π140π	122σ126π130π-132π133π134π	120π126π130π-132π133π137π
2 (139)	131π133π135π-142π143π145π	131π133π134σ-140π141π145π	130σ133σ137π-140π141π145π	127π128π137π-140π141π145π
3 (135)	127π129π131π-137π138π140π	127π129π130σ-136π141π144σ	129π131π133π-136π137π140σ	129π131π133π-136π137π138π
4 (135)	130π131π133π-138π140π141π	126σ127π129σ-136π137π141π	126σ130σ133π-136π137π138σ	124π130π133π-136π137π141π
5 (139)	133π134π135π-142π144π145π	132π133σ134σ-140π141π145π	133σ135π138π-140π141π142σ	133π135π138π-140π141π145π
6 (139)	134π135π137π-141π142π143π	131π133σ134σ-140π145π148σ	130σ135π137π-140π141π142σ	126π135π137π-140π141π142π
7 (135)	130π131π134π-138π139π141π	129σ130σ131σ-136π141π144σ	130σ131π134π-136π137π139σ	123π131π134π-136π137π141π
8 (135)	130π131π134π-137π138π140π	127π129σ131σ-136π141π144σ	130π131π134π-136π137π138σ	130π131π134π-136π137π141π
9 (139)	134π135π138π-143π144π145π	131π133σ134σ-140π141π145π	130σ135π138π-140π141π143σ	128π135π138π-140π141π145π
10 (135)	129π130π131π-137π139π140π	129σ130π131σ-136π141π144σ	126σ130π134π-136π137π139π	124π130π134π-136π137π141π
11 (143)	132σ137π139π-146π148π149σ	136π137σ138σ-144π145π149π	134σ137σ141π-144π145π149π	130π132π141π-144π145π149π
12 (139)	132π133π135π-141π142π144π	132π133π134σ-140π145π148σ	133σ135π138π-140π141π144σ	133π135π138π-140π141π142π
13 (139)	134π135π138π-143π144π145π	130σ132π133σ-140π141π145π	130σ134π138π-140π141π143π	128π134π138π-140π141π145π
14 (143)	137π138π139π-147π148π149π	136π137σ138σ-144π145π149π	137σ139π142π-144π145π147σ	137π139π142π-144π145π149π
15 (143)	138π139π142π-145π146π148π	135π137σ138σ-144π149π153σ	134σ139π142π-144π145π146σ	132π139π142π-144π145π146π
16 (139)	134π135π138π-143π144π145π	133σ134σ135σ-140π145π148σ	134σ135π138π-140π141π144σ	128π135π138π-140π141π145π
17 (139)	134π135π138π-141σ143π144π	133σ134π135σ-140π145π148π	134π135π138π-140π141π143π	134π135π138π-140π141π145π
18 (143)	138π139π142π-147π148π149π	136π137σ138σ-144π145π149π	134σ139π142π-144π145π147σ	133π139π142π-144π145π149π
19 (139)	133π134π135π-141π142π144π	133σ134π135σ-140π145π148σ	129σ134π137π-140π141π142π	126π134π137π-140π141π145π

20 (147)	140π141π143π-150π151π153σ	139π141π142σ-148π149π153π	137σ141σ144π-148π149π153π	133π134π144π-148π149π153π
21 (143)	135π137π139π-145π146π148π	135π137π138σ-144π149π152π	137π139π140π-144π145π148σ	137π139π140π-144π145π146π
22 (143)	138π139π141π-147π148π149π	133σ135π137σ-144π145π149π	133σ138σ141π-144π145π147σ	130π138π141π-144π145π149π
23 (147)	141π142π143π-151π152π153π	139π141σ142σ-148π149π153π	141σ143π145π-148π149π151σ	141π143π145π-148π149π153π
24 (147)	142π143π145π-149π150π151π	139π140σ142σ-148π153π156σ	137σ143π145π-148π149π150σ	133π143π145π-148π149π150π
25 (143)	138π139π141π-146π148π149π	137σ138σ139σ-144π149π151σ	138139π141π-144π145π148π	130π139π141π-144π145π149π
26 (143)	138π139π141π-145π146π148π	137σ138σ139σ-144π149π152σ	138π139π141π-144π145π146π	138π139π141π-144π145π149π
27 (147)	143π145π146π-151π152π153π	139π141σ142σ-148π149π153π	143π145π146π-148π149π151σ	143π145π146π-148π149π153π

Table 7: Local molecular orbitals of atoms 19, 21, 24 and 26

Mol.	Atom 19	Atom 21	Atom 24	Atom 26
1 (131)	122σ123σ125σ-147σ150σ152σ	123σ129σ131σ-150σ151σ152σ	121σ129σ131σ-148σ151σ155σ	124σ129σ131σ-139σ145σ151σ
2 (139)	130σ131σ134σ-149σ156σ159σ	131σ138σ139σ-159σ160σ161σ	129σ138σ139σ-158σ164σ165σ	132σ138σ139σ-148σ153σ160σ
3 (135)	126σ127σ130σ-151σ154σ156σ	127σ134σ135σ-154σ155σ156σ	125σ134σ135σ-152σ153σ155σ	128σ134σ135σ-143σ149σ155σ
4 (135)	126σ127σ129σ-150σ155σ157σ	127σ134σ135σ-155σ157σ159σ	125σ134σ135σ-151σ152σ154σ	128σ134σ135σ-143σ144σ148σ
5 (139)	130σ132σ134σ-151σ156σ158σ	132σ137σ139σ-160σ161σ164σ	129σ137σ139σ-157σ160σ164σ	131σ137σ139σ-147σ153σ160σ
6 (139)	131σ133σ134σ-156σ157σ159σ	131σ138σ139σ-159σ160σ161σ	129σ138σ139σ-157σ158σ161σ	132σ138σ139σ-149σ150σ153σ
7 (135)	127σ129σ130σ-151σ154σ156σ	127σ133σ135σ-154σ155σ157σ	125σ133σ135σ-152σ153σ155σ	128σ133σ135σ-143σ144σ145σ
8 (135)	126σ127σ129σ-151σ154σ155σ	127σ133σ135σ-155σ158σ160σ	125σ133σ135σ-152σ153σ159σ	128σ133σ135σ-143σ148σ156σ
9 (139)	130σ131σ133σ-156σ159σ162σ	131σ137σ139σ-159σ161σ162σ	129σ137σ139σ-157σ160σ165σ	132σ137σ139σ-147σ153σ160σ
10 (135)	126σ128σ129σ-147σ151σ154σ	128σ133σ135σ-154σ155σ159σ	125σ133σ135σ-152σ155σ159σ	127σ133σ135σ-143σ148σ154σ
11 (143)	134σ136σ138σ-160σ163σ165σ	136σ142σ143σ-163σ164σ165σ	133σ142σ143σ-161σ164σ168σ	135σ142σ143σ-152σ157σ164σ
12 (139)	130σ132σ134σ-155σ158σ160σ	132σ137σ139σ-158σ159σ160σ	129σ137σ139σ-156σ159σ163σ	131σ137σ139σ-147σ153σ159σ
13 (139)	130σ132σ133σ-151σ155σ157σ	132σ137σ139σ-159σ160σ161σ	129σ137σ139σ-156σ158σ159σ	131σ137σ139σ-147σ152σ159σ
14 (143)	134σ136σ138σ-154σ155σ160σ	136σ141σ143σ-165σ168σ169σ	132σ141σ143σ-161σ163σ164σ	135σ141σ143σ-151σ157σ164σ
15 (143)	135σ137σ138σ-159σ160σ162σ	135σ141σ143σ-163σ164σ165σ	133σ141σ143σ-161σ162σ164σ	136σ141σ143σ-152σ157σ164σ
16 (139)	132σ133σ134σ-155σ158σ160σ	132σ137σ139σ-158σ159σ163σ	129σ137σ139σ-156σ159σ163σ	131σ137σ139σ-147σ153σ159σ
17 (139)	130σ132σ133σ-151σ155σ158σ	132σ137σ139σ-159σ162σ164σ	129σ137σ139σ-156σ157σ160σ	131σ137σ139σ-147σ152σ160σ
18 (143)	134σ136σ137σ-155σ160σ163σ	136σ141σ143σ-163σ164σ166σ	133σ141σ143σ-161σ164σ167σ	135σ141σ143σ-151σ157σ164σ

19 (139)	129σ131σ133σ-148σ155σ159σ	131σ138σ139σ-159σ165σ166σ	136σ138σ139σ-156σ158σ160σ	132σ136σ139σ-147σ153σ160σ
20 (147)	137σ139σ142σ-164σ168σ169σ	139σ146σ147σ-168σ169σ170σ	145σ146σ147σ-165σ167σ170σ	140σ145σ147σ-157σ161σ169σ
21 (143)	133σ135σ138σ-152σ159σ163σ	135σ142σ143σ-163σ164σ165σ	141σ142σ143σ-160σ162σ169σ	136σ141σ143σ-151σ152σ157σ
22 (143)	133σ135σ137σ-159σ161σ164σ	135σ142σ143σ-164σ169σ171σ	140σ142σ143σ-160σ162σ163σ	136σ140σ143σ-151σ152σ156σ
23 (147)	138σ139σ142σ-164σ170σ172σ	139σ146σ147σ-170σ175σ177σ	144σ146σ147σ-165σ166σ168σ	140σ144σ147σ-155σ161σ169σ
24 (147)	139σ140σ142σ-156σ163σ166σ	144σ146σ147σ-168σ169σ170σ	144σ146σ147σ-164σ165σ167σ	141σ144σ147σ-157σ161σ170σ
25 (143)	135σ137σ138σ-159σ163σ165σ	135σ142σ143σ-163σ166σ169σ	140σ142σ143σ-160σ162σ169σ	136σ140σ143σ-152σ157σ164σ
26 (143)	133σ135σ137σ-159σ162σ164σ	135σ142σ143σ-164σ167σ171σ	140σ142σ143σ-160σ163σ169σ	136σ140σ143σ-151σ156σ165σ
27 (147)	137σ139σ141σ-164σ168σ172σ	137σ139σ147σ-168σ169σ172σ	144σ146σ147σ-165σ167σ170σ	140σ144σ147σ-155σ161σ170σ

Table 8: Local molecular orbitals of atoms 33, 37 and 40

Mol.	Atom 33	Atom 37	Atom 40
1 (131)	128π129π131π-135π138π139π	128π129π131π-135π138π139π	102σ106σ109σ-144σ145σ150σ
2 (139)	136π138π139π-144π146π148π	136π138π139π-144π146π148π	114σ115σ127σ-147σ154σ159σ
3 (135)	132π134π135π-139π142π143π	132π134π135π-139π142π143π	103σ109σ114σ-148σ152σ156σ
4 (135)	132π134π135π-139π142π143π	132π134π135π-139π142π143π	105σ115σ116σ-149σ151σ152σ
5 (139)	136π137π139π-143π146π147π	136π137π139π-143π146π147π	114σ122σ125σ-152σ154σ156σ
6 (139)	136π138π139π-144π147π148π	136π138π139π-144π147π148π	134π135π137π-142π146σ155σ
7 (135)	132π133π135π-140π142π143π	132π133π135π-140π142π143π	130π131π134π-138π139π141π
8 (135)	132π133π135π-139π142π143π	132π133π135π-139π142π143π	114σ116σ130σ-138σ149σ155π
9 (139)	136π137π139π-142π146π147π	136π137π139π-142π146π147π	128π135π138π-143π144π145π
10 (135)	124σ127π132π-138π142π143π	132π133π135π-138π142π143π	104σ107σ114σ-149σ153σ156σ
11 (143)	131σ135π140π-147π151π152π	140π142π143π-147π151π152π	118σ119σ120σ-150σ158σ162σ
12 (139)	128σ131π136π-143π146π147π	136π137π139π-143π146π147π	107σ113σ119σ-152σ157σ160σ
13 (139)	127σ131π136π-142π146π147π	136π137π139π-142π146π147π	110σ120σ121σ-153σ155σ156σ
14 (143)	131σ135π140π-146π150π151π	140π141π143π-146π150π151π	125σ129σ130σ-156σ157σ158σ
15 (143)	133σ136π140π-147π151π152π	140σ141π143π-147π151π152π	138π139π142π-146π150σ160σ
16 (139)	129σ131π136π-142π146π147π	136π137π139π-142π146π147π	134π135π138π-143π144π145π
17 (139)	127σ131π136π-142π146π147π	136π137π139π-142π146π147π	118σ121σ134σ-143σ153σ159π
18 (143)	131σ135π140π-	140π141π143π-	133π139π142π-

	146π150π151π	146π150π151π	147π148π149π
19 (139)	132π136π138π-143π146π147π	136π138π139π-143π146π147π	109σ113σ117σ-152σ153σ157σ
20 (147)	140π145π146π-152π155π156π	145π146π147π-152π155π156π	120σ121σ134σ-154σ162σ168σ
21 (143)	136π141π142π-147π150π151π	141π142π143π-147π150π151π	108σ116σ122σ-156σ161σ165σ
22 (143)	136π140π142π-146π150π151π	140π142π143π-146π150π151π	112σ122σ123σ-156σ157σ160σ
23 (147)	140π144π146π-150π154π155π	144π146π147π-150π154π155π	121σ128σ132σ-160σ163σ167σ
24 (147)	141π144π146π-152π155π157π	144π146π147π-152π155π157π	142π143π145π-150π154σ164σ
25 (143)	136π140π142π-147π150π152π	140π142π143π-147π150π151π	138π139π141π-146π148π149π
26 (143)	136π140π142π-147π150π151π	140π142π143π-147π150π151π	121σ123σ138σ-146σ157σ164σ
27 (147)	144π145π146π-150π154π155π	145π146π147π-150π154π155π	143π145π146π-151π152π153π

Discussion

Discussion of 5-HT_{1A} receptor affinity results [67]

Table 2 shows that the importance of variables in Eq. 1 is S_{33}^{E}(HOMO-2)*>> S_{40}^{N}(LUMO+2)*> S_{6}^{N}(LUMO+1)*> S_{19}^{N}(LUMO)*. A high receptor binding affinity is associated with large (negative) values of S_{33}^{E}(HOMO-2)*, large (positive) values of S_{40}^{N}(LUMO+2)*, small (positive) values of S_{6}^{N}(LUMO+1)* and small (positive) values of S_{19}^{N}(LUMO)*.Atom 33 is a carbon shared by rings E and F (Fig. 2). A high receptor binding affinity is associated with large negative values of S_{33}^{E}(HOMO-2)*. Table 8 shows that the three highest occupied local MOs have a π nature in all molecules. Large (negative) values of S_{33}^{E}(HOMO-2)* are obtained by shifting the MO energy toward zero, increasing the reactivity of this MO [67]. With this procedure, $(\text{HOMO-1})_{33}^{*}$ and $(\text{HOMO})_{33}^{*}$ also increase their reactivity. This suggests that atom 33 is interacting with the site through π-cation or π-π (stacked or T-shaped) interactions. Atom 40 corresponds to the atom bonded to atom 1 of ring A (Fig. 2). Table 1 shows that this atom could be H, Cl, F, C or O. Large (positive) values of S_{40}^{N}(LUMO+2)* are obtained by shifting the eigenvalue toward zero, making this MO more reactive. In this case, $(\text{LUMO-1})_{40}^{*}$ and $(\text{LUMO})_{40}^{*}$ also become more reactive. On the other hand, Table 8 shows that the three lowest empty MOs have a σ or π nature. In all molecules $(\text{LUMO})_{40}^{*}$ does not coincide with the molecular LUMO. In some cases $(\text{LUMO})_{40}^{*}$ coincides with empty MOs that are energetically very far from the molecule's LUMO. The different nature of the empty MOs, suggests the possibility of the existence of more than one mechanism involved in the atom_{40}-site interaction. If this is the case, π MOs could interact with anion(s), with lone pairs of with occupied π MOs from the site. σ MOs can interact with one or more alkyl chains. Atom 6 is a carbon in ring A (Fig. 2). A high receptor binding affinity is associated with small (positive) values of S_{6}^{N}(LUMO+1)*. Small values of this reactivity index are obtained by shifting upwards the corresponding eigenvalue, making this MO less reactive. Table 6 shows that the three lowest empty MOs have a π nature and that the frontier local MOs do not coincide with the molecule's frontier molecular orbitals. The energy of $(\text{LUMO})_{6}^{*}$ is very close to the energy of $(\text{LUMO+1})_{6}^{*}$. Then, we may suggest that a better affinity could be also associated with a less reactive $(\text{LUMO})_{6}^{*}$. If this is the case, then atom 6 can be considered as a weak electron-rich center (see Table 6). In this case, it can interact with the site through π-π (stacked or T-shaped), π-σ or π-cation interactions. Atom 19 is a sp^3 carbon forming part of the chain linking rings C and D (Fig. 2). Small (positive) values of S_{19}^{N}(LUMO)* are associated with high receptor affinity. Table 7 shows that all local MOs have a σ nature. Small values for this reactivity index will lower its reactivity. Therefore, atom-site interaction should be through at least $(HOMO)_{19}^{*}$, suggesting an that atom 19 interacts with an aliphatic amino acid side-chain (alkyl-alkyl interaction).All the suggestions are displayed in the partial 2D pharmacophore of Fig. 5.

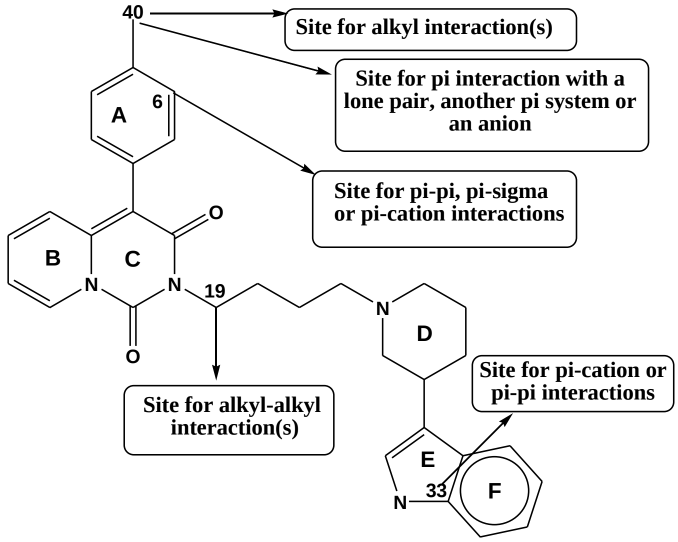

Figure 5: Partial 2D pharmacophore for 5-HT$_{1A}$ receptor affinity

Discussion of serotonin transporter protein (SERT) affinity results

Table 4 shows that the importance of variables in Eq. 2 is S_{26}^{N}(LUMO+2)*~ S_{13}^{E}(HOMO-1)*>S_{21}^{N}(LUMO+1)*>S_{37}^{E}(HOMO)*>μ_{10}>>F_{10}(LUMO+1)*~ S_{24}^{N}(LUMO)*>F_{15}(HOMO-2)*.The analysis of equation 2 shows that a high SERT affinity is associated with large (negative) values of S_{13}^{E}(HOMO-1)*, small (negative) values of S_{37}^{E}(HOMO)*, small (positive) values of S_{21}^{N}(LUMO+1)*, small (positive) values of S_{26}^{N}(LUMO+2)*, small (negative) values of μ_{10}, large values of F_{10}(LUMO+1)*, large (positive) values of S_{24}^{N}(LUMO)* and small values of F_{15}(HOMO-2)*. Atom 26 is a sp^3 carbon in ring D (Fig. 2). A high SERT affinity is associated with small (positive) values of S_{26}^{N}(LUMO+2)*. These small values are obtained faster by enlarging the energy of $(LUMO+2)_{26}^{*}$, making it less reactive. Table 7 shows that $(LUMO+2)_{26}^{*}$ corresponds to empty molecular MOs that are energetically very far from the LUMO. Therefore we may discard the interaction of atom 26 with one or more electron-rich centers. On the other hand, Table 7 also shows that the local $(HOMO)_{26}^{*}$ coincides with the molecular HOMO in all cases. This suggests a σ-σ interaction (an alkyl interaction with aliphatic amino acid side-chains). Atom 13 is a carbon in ring B (Fig. 2). A high SERT affinity is associated with large (negative) values of S_{13}^{E}(HOMO-1)*. Table 6 shows that $(HOMO)_{13}^{*}$ has a π nature and that it does not coincide with the molecular HOMO in all cases. $(HOMO-1)_{13}^{*}$ has σ or π natures (Table 6). Now, we know that large negative values are obtained by shifting the MO energy toward zero, making it more reactive[67]. And this process will also make $(HOMO)_{13}^{*}$more reactive. This suggests that an ideal situation is when $(HOMO)_{13}^{*}$ and $(HOMO-1)_{13}^{*}$ coincide with the molecular HOMO and (HOMO-1). Regarding the kind of interactions, the π nature of $(HOMO)_{13}^{*}$ suggests that atom 13 could be engaged in a π-π or π-alkyl interactions with the site involving all or part of ring B. This last interaction could explain the involvement of σ MOs. Atom 21 is a sp^3 carbon in the chain linking rings C and D (Fig. 2). A high SERT affinity is associated with small (positive) values of S_{21}^{N}(LUMO+1)*. Table 7 shows that all MOs have a σ nature, that $(HOMO)_{21}^{*}$ coincides with the molecular HOMO in all cases and that $(LUMO)_{21}^{*}$ is energetically very far from the corresponding molecular LUMO. Small values of S_{21}^{N}(LUMO+1)* shows that this atom is not interacting with electron-rich moieties. Therefore we suggest that atom 21 is engaged in one or more alkyl interactions with aliphatic amino acid side-chains. Atom 37 is a carbon in ring F (Fig. 2). A high SERT affinity is associated with small (negative) values of S_{37}^{E}(HOMO)*. As these small values are obtained by making this MO less reactive the ideal situation occurs when $(HOMO)_{37}^{*}$ does not coincide with the molecular HOMO (see Table 8) [67]. This suggests that atom 37 could be facing an electron-rich center. Now, considering that the three highest occupied local MOs and the three lowest empty local MOs have a π nature (Table 8), it is possible to suggest that atom 37 could be interacting with another π center through its empty local MOs or with an anion (π-anion interaction). Atom 10 is nitrogen in ring C (Fig. 2). A high SERT affinity is associated with small (negative) values of μ_{10}. This index corresponds to the midpoint of the $(HOMO)_{10}*$ and $(LUMO)_{10}^{*}$ energies. Table 6 shows that $(LUMO)_{10}^{*}$ coincides with the molecular LUMO in all cases. It also shows that $(HOMO)_{10}*$ does not coincide with the molecule's HOMO. Smaller negative values can be obtained by shifting toward zero the $(HOMO)_{10}*$. This shifting is carried out, not by changing the actual $(HOMO)_{10}*$, but by adding substituents to the molecule in such a way that the new $(HOMO)_{10}*$ coincides with the molecular HOMO. Given the σ nature of $(HOMO)_{10}*$ it is suggested that atom 10 is probably interacting with a cation or with another electron-deficient center. On the other hand a high SERT affinity is also associated with large values of $F_{10}(LUMO+1)*$ indicating that $(LUMO+1)_{10}^{*}$ and $(LUMO)_{10}^{*}$ are also engaged in an interaction with an electron-rich center situated in the site (for example an anion).Atom 24 is a sp^3 carbon in ring D (Fig. 2). A high SERT affinity is associated with large (positive) values of $S_{24}^{N}(LUMO)*$. Table 7 shows that $(LUMO)_{24}^{*}$ corresponds, in general, to an empty molecular orbital that is energetically very distant from the molecular LUMO. Higher positive values for this index are obtained by shifting the energy of the corresponding MO toward zero. Therefore, the ideal situation is when the molecular LUMO is localized on atom 24 (i.e., $(LUMO)_{24}^{*}$ coincides with the molecular LUMO). This suggests that atom 24 is interacting with an electron-rich moiety through σ-π or alkyl interactions. Atom 15 is a carbon in ring B (Fig. 2). A high SERT affinity is associated with small (positive) values of $F_{15}(HOMO-2)*$. Table 6 shows that all occupied and empty local MOs have a π nature. Small values for this index are obtained by lowering the localization of $(HOMO-2)_{15}^{*}$ on this atom (i.e., by lowering the electron population of this MO on this atom [67]). If this requirement holds also for $(HOMO-1)_{15}^{*}$ and $(HOMO)_{15}^{*}$ this atom should behave as a bad electron donor. This suggests that atom 15 is interacting with an electron-rich center through π-π orπ-alkyl interactions like atom 13. All the suggestions are displayed in the partial 2D pharmacophore of Fig. 6.

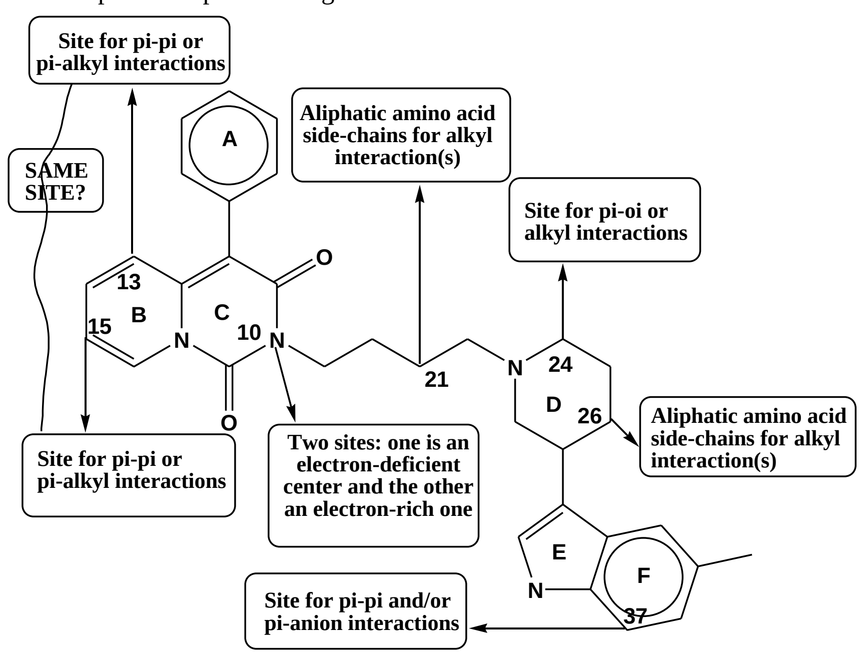

Figure 6: Partial 2D pharmacophore for the serotonin transporter protein affinity

In summary, we have found a statistically significant relationship between the electronic structure and the $5\text{-}HT_{1A}$ receptor affinity. The KPG method also allowed obtaining a statistically significant relationship between the electronic structure and the serotonin transporter protein affinity. This data allowed building the corresponding 2D pharmacophores. These structures could help the experimentalists in the development of more potent molecules.

References

[1]. Metts, A. V.; Rubin-Falcone, H.; Ogden, R. T.; Lin, X.; Wilner, D. E.; Burke, A. K.; Sublette, M. E.; Oquendo, M. A.; Miller, J. M.; Mann, J. J. Antidepressant medication exposure and 5-HT1A autoreceptor binding in major depressive disorder. *Synapse* 2019, 73, e22089.

[2]. Depoortère, R.; Bardin, L.; Varney, M. A.; Newman-Tancredi, A. Serotonin 5-HT1A Receptor Biased Agonists Display Differential Anxiolytic Activity in a Rat Social Interaction Model. *ACS Chemical Neuroscience* 2019.

[3]. Albert, P. R.; Vahid-Ansari, F. The 5-HT1A receptor: Signaling to behavior. *Biochimie* 2019, 161, 34-45.

[4]. Staroń, J.; Bugno, R.; Hogendorf, A. S.; Bojarski, A. J. 5-HT1A receptor ligands and their therapeutic applications: review of new patents. *Expert Opinion on Therapeutic Patents* 2018, 28, 679-689.

[5]. Segi-Nishida, E. The Effect of Serotonin-Targeting Antidepressants on Neurogenesis and Neuronal Maturation of the Hippocampus Mediated via 5-HT1A and 5-HT4 Receptors. *Frontiers in Cellular Neuroscience* 2017, 11.

[6]. Glikmann-Johnston, Y.; Saling, M. M.; Reutens, D. C.; Stout, J. C. Hippocampal 5-HT1A Receptor and Spatial Learning and Memory. *Frontiers in Pharmacology* 2015, 6.

[7]. Sarkar, P.; Kumar, G. A.; Pal, S.; Chattopadhyay, A. Chapter 1 - Biophysics of Serotonin and the Serotonin1A Receptor: Fluorescence and Dynamics. In *Serotonin*, Pilowsky, P. M., Ed. Academic Press: Boston, 2019; pp 3-22.

[8]. Beecher, K.; Belmer, A.; Bartlett, S. E. Chapter 6 - Anatomy of the Serotonin Transporter. In *Serotonin*, Pilowsky, P. M., Ed. Academic Press: Boston, 2019; pp 121-133.

[9]. Zaręba, P.; Jaśkowska, J.; Śliwa, P.; Satała, G. New dual ligands for the D2 and 5-HT1A receptors from the group of 1,8-naphthyl derivatives of LCAP. *Bioorganic & Medicinal Chemistry Letters* 2019.

[10]. Gu, Z.S.; Zhou, A.-n.; Xiao, Y.; Zhang, Q.W.; Li, J.Q. Synthesis and antidepressant-like activity of novel aralkyl piperazine derivatives targeting SSRI/5-HT_{1A}/5-HT_7. *European Journal of Medicinal Chemistry* 2018, 144, 701-715.

[11]. Franchini, S.; Bencheva, L. I.; Battisti, U. M.; Tait, A.; Sorbi, C.; Fossa, P.; Cichero, E.; Ronsisvalle, S.; Aricò, G.; Denora, N.; Iacobazzi, R. M.; Cilia, A.; Pirona, L.; Brasili, L. Synthesis and biological evaluation of 1,3-dioxolane-based 5-HT_{1A} receptor agonists for CNS disorders and neuropathic pain. *Future Medicinal Chemistry* 2018, 10, 2137-2154.

[12]. Ostrowska, K.; Młodzikowska, K.; Głuch-Lutwin, M.; Gryboś, A.; Siwek, A. Synthesis of a new series of aryl/heteroarylpiperazinyl derivatives of 8-acetyl-7-hydroxy-4-methylcoumarin with low nanomolar 5-HT_{1A} affinities. *European Journal of Medicinal Chemistry* 2017, 137, 108-116.

[13]. Franchini, S.; Manasieva, L. I.; Sorbi, C.; Battisti, U. M.; Fossa, P.; Cichero, E.; Denora, N.; Iacobazzi, R. M.; Cilia, A.; Pirona, L.; Ronsisvalle, S.; Aricò, G.; Brasili, L. Synthesis, biological evaluation and molecular modeling of 1-oxa-4-thiaspiro- and 1,4-dithiaspiro[4.5]decane derivatives as potent and selective 5-HT_{1A} receptor agonists. *European Journal of Medicinal Chemistry* 2017, 125, 435-452.

[14]. Fiorino, F.; Magli, E.; Kędzierska, E.; Ciano, A.; Corvino, A.; Severino, B.; Perissutti, E.; Frecentese, F.; Di Vaio, P.; Saccone, I.; Izzo, A. A.; Capasso, R.; Massarelli, P.; Rossi, I.; Orzelska-Gòrka, J.; Kotlińska, J. H.; Santagada, V.; Caliendo, G. New 5-HT1A, 5HT2A and 5HT2C receptor ligands containing a picolinic nucleus: Synthesis, in vitro and in vivo pharmacological evaluation. *Bioorganic & Medicinal Chemistry* 2017, 25, 5820-5837.

[15]. Ofori, E.; Zhu, X. Y.; Etukala, J. R.; Peprah, K.; Jordan, K. R.; Adkins, A. A.; Bricker, B. A.; Kang, H. J.; Huang, X.-P.; Roth, B. L.; Ablordeppey, S. Y. Design and synthesis of dual 5-HT_{1A} and 5-HT_7 receptor ligands. *Bioorganic & Medicinal Chemistry* 2016, 24, 3464-3471.

[16]. Kaufman, J.; DeLorenzo, C.; Choudhury, S.; Parsey, R. V. The 5-HT_{1A} receptor in Major Depressive Disorder. *European Neuropsychopharmacology* 2016, 26, 397-410.

[17]. Heinrich, T.; Böttcher, H.; Gericke, R.; Bartoszyk, G. D.; Anzali, S.; Seyfried, C. A.; Greiner, H. E.; van Amsterdam, C. Synthesis and Structure−Activity Relationship in a Class of Indolebutylpiperazines as Dual 5-HT1A Receptor Agonists and Serotonin Reuptake Inhibitors. *Journal of Medicinal Chemistry* 2004, 47, 4684-4692.

[18]. Brinkø, A.; Larsen, M. T.; Koldsø, H.; Besenbacher, L.; Kolind, A.; Schiøtt, B.; Sinning, S.; Jensen, H. H. Synthesis and inhibitory evaluation of 3-linked imipramines for the exploration of the S2 site of the human serotonin transporter. *Bioorganic & Medicinal Chemistry* 2016, 24, 2725-2738.

[19]. Toda, N.; Kaneko, T.; Kogen, H. Development of an efficient therapeutic agent for Alzheimer's disease: design and synthesis of dual inhibitors of acetylcholinesterase and serotonin transporter. *Chemical and Pharmaceutical Bulletin* 2010, 58, 273-287.

[20]. Koldsø, H.; Severinsen, K.; Tran, T. T.; Celik, L.; Jensen, H. H.; Wiborg, O.; Schiøtt, B.; Sinning, S. The two enantiomers of citalopram bind to the human serotonin transporter in reversed orientations. *Journal of the American Chemical Society* 2010, 132, 1311-1322.

[21]. Banala, A. K.; Zhang, P.; Plenge, P.; Cyriac, G.; Kopajtic, T.; Katz, J. L.; Loland, C. J.; Newman, A. H. Design and synthesis of 1-(3-(dimethylamino) propyl)-1-(4-fluorophenyl)-1, 3-dihydroisobenzofuran-5-carbonitrile (citalopram) analogues as novel probes for the serotonin transporter S1 and S2 binding sites. *Journal of Medicinal Chemistry* 2013, 56, 9709-9724.

[22]. Nencetti, S.; Mazzoni, M. R.; Ortore, G.; Lapucci, A.; Giuntini, J.; Orlandini, E.; Banti, I.; Nuti, E.; Lucacchini, A.; Giannaccini, G. Synthesis, molecular docking and binding studies of selective serotonin transporter inhibitors. *European Journal of Medicinal Chemistry* 2011, 46, 825-834.

[23]. Gómez-Jeria, J. S.; Castro-Latorre, P.; Moreno-Rojas, C. Dissecting the drug-receptor interaction with the Klopman-Peradejordi-Gómez (KPG) method. II. The interaction of 2,5-dimethoxyphenethylamines and their N-2-methoxybenzyl-substituted analogs with 5-HT_{2A} serotonine receptors. *Chemistry Research Journal* 2018, 4, 45-62.

[24]. Gómez-Jeria, J. S.; Moreno-Rojas, C. Dissecting the drug-receptor interaction with the Klopman-Peradejordi-Gómez (KPG) method. I. The interaction of 2,5-dimethoxyphenethylamines and their N-2-methoxybenzyl-substituted analogs with 5-HT1A serotonine receptors. *Chemistry Research Journal* 2017, 2, 27-41.

[25]. Gómez-Jeria, J. S.; Becerra-Ruiz, M. B. Electronic structure and rat fundus serotonin receptor binding affinity of phenetylamines and indolealkylamines. *International Journal of Advances in Pharmacy, Biology and Chemistry* 2017, 6, 72-86.

[26]. Gómez-Jeria, J. S.; Cassels, B. K.; Saavedra-Aguilar, J. C. A quantum-chemical and experimental study of the hallucinogen (±)-1-(2,5-dimethoxy-4-nitrophenyl)-2-aminopropane (DON). *European Journal of Medicinal Chemistry* 1987, 22, 433-437.

[27]. Gómez-Jeria, J. S.; Morales-Lagos, D.; Cassels, B. K.; Saavedra-Aguilar, J. C. Electronic structure and serotonin receptor binding affinity of 7-substituted tryptamines. *Quantitative Structure-Activity Relationships* 1986, 5, 153-157.

[28]. Gómez-Jeria, J. S.; Morales-Lagos, D.; Rodriguez-Gatica, J. I.; Saavedra-Aguilar, J. C. Quantum-chemical study of the relation between electronic structure and pA2 in a series of 5-substituted tryptamines. *International Journal of Quantum Chemistry* 1985, 28, 421-428.

[29]. Gómez-Jeria, J. S.; Morales-Lagos, D. R. Quantum chemical approach to the relationship between molecular structure and serotonin receptor binding affinity. *Journal of Pharmaceutical Sciences* 1984, 73, 1725-1728.

[30]. Gómez Jeria, J. S. La Pharmacologie Quantique. *Bollettino Chimico Farmaceutico* 1982, 121, 619-625.

[31]. Gómez-Jeria, J. S.; Robles-Navarro, A. A Note on the Docking of some Hallucinogens to the 5-HT_{2A} Receptor. *Journal of Computational Methods in Molecular Design* 2015, 5, 45-57.

[32]. Richter, P.; Morales, A.; Gomez-Jeria, J. S.; Morales-Lagos, D. Electrochemical study of the hallucinogen (±)-1-(2,5-dimethoxy-4-nitrophenyl)-2-aminopropane. *Analyst* 1988, 113, 859-863.

[33]. Gómez-Jeria, J. S.; Cassels, B. K.; Clavijo, R. E.; Vargas, V.; Quintana, R.; Saavedra-Aguilar, J. C. Spectroscopic characterization of a new hallucinogen: 1-(2,5-dimethoxy-4-nitrophenyl)-2-aminipropane (DON). *Microgram (DEA)* 1986, 19, 153-162.

[34]. Gómez-Jeria, J. S. Approximate Molecular Electrostatric Potentials of Protonated Mescaline Analogues. *Acta sud Americana de Química* 1984, 4, 1-9.

[35]. Gómez-Jeria, J. S.; Morales-Lagos, D. The mode of binding of phenylalkylamines to the Serotonergic Receptor. In *QSAR in design of Bioactive Drugs*, Kuchar, M., Ed. Prous, J.R.: Barcelona, Spain, 1984; pp 145-173.

[36]. Gómez-Jeria, J. S.; Robles-Navarro, A. A Quantum Chemical Study of the Relationships between Electronic Structure and cloned rat 5-HT_{2C} Receptor Binding Affinity in N-Benzylphenethylamines. *Research Journal of Pharmaceutical, Biological and Chemical Sciences* 2015, 6, 1358-1373.

[37]. Gómez-Jeria, J. S.; Abuter-Márquez, J. A Theoretical Study of the Relationships between Electronic Structure and 5-HT_{1A} and 5- HT_{2A} Receptor Binding Affinity of a group of ligands containing an isonicotinic nucleus. *Chemistry Research Journal* 2017, 2, 198-213.

[38]. Gómez-Jeria, J. S.; Moreno-Rojas, C.; Castro-Latorre, P. A note on the binding of N-2-methoxybenzyl-phenethylamines (NBOMe drugs) to the 5-HT_{2C} receptors. *Chemistry Research Journal* 2018, 3, 169-175.

[39]. Ślifirski, G.; Król, M.; Kleps, J.; Ulenberg, S.; Belka, M.; Bączek, T.; Siwek, A.; Stachowicz, K.; Szewczyk, B.; Nowak, G.; Bojarski, A.; Kozioł, A. E.; Turło, J.; Herold, F. Synthesis of novel pyrido[1,2-c]pyrimidine derivatives with rigidized tryptamine moiety as potential SSRI and 5-HT1A receptor ligands. *European Journal of Medicinal Chemistry* 2019, 166, 144-158.

[40]. Important. Given that the methodology used here has been employed in more than 50 papers, we have adopted a standard way to present some aspects of the research. Some phrases are stantard to all our papers because they cannot be written in infinite different ways. Do not confuse this with self plagiarism.

[41]. All papers of J.S. G.-J. can be found in https://www.researchgate.net/profile/Juan-Sebastian_Gomez-Jeria.

[42]. Gómez-Jeria, J. S. On some problems in quantum pharmacology I. The partition functions. *International Journal of Quantum Chemistry* 1983, 23, 1969-1972.

[43]. Gómez-Jeria, J. S. Modeling the Drug-Receptor Interaction in Quantum Pharmacology. In *Molecules in Physics, Chemistry, and Biology*, Maruani, J., Ed. Springer Netherlands: 1989; Vol. 4, pp 215-231.

[44]. Gómez-Jeria, J. S.; Ojeda-Vergara, M. Parametrization of the orientational effects in the drug-receptor interaction. *Journal of the Chilean Chemical Society* 2003, 48, 119-124.

[45]. Alarcón, D. A.; Gatica-Díaz, F.; Gómez-Jeria, J. S. Modeling the relationships between molecular structure and inhibition of virus-induced cytopathic efects. Anti-HIV and anti-H1N1 (Influenza) activities as examples. *Journal of the Chilean Chemical Society* 2013, 58, 1651-1659.

[46]. Gómez-Jeria, J. S. *Elements of Molecular Electronic Pharmacology (in Spanish)*. 1st ed.; Ediciones Sokar: Santiago de Chile, 2013; p 104.

[47]. Gómez-Jeria, J. S. A New Set of Local Reactivity Indices within the Hartree-Fock-Roothaan and Density Functional Theory Frameworks. *Canadian Chemical Transactions* 2013, 1, 25-55.

[48]. Gómez-Jeria, J. S.; Flores-Catalán, M. Quantum-chemical modeling of the relationships between molecular structure and in vitro multi-step, multimechanistic drug effects. HIV-1 replication inhibition and inhibition of cell proliferation as examples. *Canadian Chemical Transactions* 2013, 1, 215-237.

[49]. Paz de la Vega, A.; Alarcón, D. A.; Gómez-Jeria, J. S. Quantum Chemical Study of the Relationships between Electronic Structure and Pharmacokinetic Profile, Inhibitory Strength toward Hepatitis C virus NS5B Polymerase and HCV replicons of indole-based compounds. *Journal of the Chilean Chemical Society* 2013, 58, 1842-1851.

[50]. Gómez-Jeria, J. S. Tables of proposed values for the Orientational Parameter of the Substituent. I. Monoatomic, Diatomic, Triatomic, n-CnH2n+1, O-n-CnH2n+1, NRR', and Cycloalkanes (with a single

ring) substituents. *Research Journal of Pharmaceutical, Biological and Chemical Sciences* 2016, 7, 288-294.

[51]. Gómez-Jeria, J. S. Tables of proposed values for the Orientational Parameter of the Substituent. II. *Research Journal of Pharmaceutical, Biological and Chemical Sciences* 2016, 7, 2258-2260.

[52]. Gómez-Jeria, J. S. 45 Years of the KPG Method: A Tribute to Federico Peradejordi. *Journal of Computational Methods in Molecular Design* 2017, 7, 17-37.

[53]. Kpotin, G. A.; Bédé, A. L.; Houngue-Kpota, A.; Anatovi, W.; Kuevi, U. A.; Atohoun, G. S.; Mensah, J.-B.; Gómez-Jeria, J. S.; Badawi, M. Relationship between electronic structures and antiplasmodial activities of xanthone derivatives: a 2D-QSAR approach. *Structural Chemistry* 2019, https://doi.org/10.1007/s11224-019-01333-w.

[54]. Gómez-Jeria, J. S.; Sánchez-Jara, B. An introductory theoretical investigation of the relationships between electronic structure and A1, A2A and A3 adenosine receptor affinities of a series of N6-8,9-trisubstituted purine derivatives. *Chemistry Research Journal* 2019, 4, 46-59.

[55]. Gómez-Jeria, J. S.; Kpotin, G. A Density Functional Theory Analysis of the relationships between electronic structure and KCNQ2 potassium channels inhibition by a series of retigabine derivatives. *Chemistry Research Journal* 2019, 4, 68-79.

[56]. Gómez-Jeria, J. S.; Gatica-Díaz, N. A preliminary quantum chemical analysis of the relationships between electronic structure and 5-HT_{1A} and 5-HT_{2A} receptor affinity in a series of 8-acetyl-7-hydroxy-4-methylcoumarin derivatives. *Chemistry Research Journal* 2019, 4, 85-100.

[57]. Gómez-Jeria, J. S.; Garrido-Sáez, N. A DFT analysis of the relationships between electronic structure and affinity for dopamine D_2, D_3 and D_4 receptor subtypes in a group of 77-LH-28-1 derivatives. *Chemistry Research Journal* 2019, 4, 30-42.

[58]. Gómez-Jeria, J. S.; Contreras-Lira, V. A DFT analysis of the relationships between electronic structure and inhibition of aurora kinase A and epidermal growth factor receptor kinase by a set of N4-phenyl substituted-7H-pyrrolo[2,3-d]pyrimidin-4-amines. *Chemistry Research Journal* 2019, 4, 34-45.

[59]. Gautier, K. S.; Kpotin, G. A.; Mensah, J.-B.; Gómez-Jeria, J. S. Quantum-Chemical Study of the Relationships between Electronic Structure and the Affinity of Benzisothiazolylpiperazine Derivatives for the Dopamine Hd2l and Hd3 Receptors. *The Pharmaceutical and Chemical Journal* 2019, 6, 73-90.

[60]. Abdussalam, A.; Gómez-Jeria, J. S. Quantum Chemical Study of the Relationships between Electronic Structure and Corticotropin-Releasing Factor 1 Receptor Binding Inhibition by a Group of Benzazole Derivatives. *Journal of Pharmaceutical and Applied Chemistry* 2019, 5, 1-9.

[61]. Kpotin, G.; Gómez-Jeria, J. S. Quantum-Chemical Study of the Relationships between Electronic Structure and Anti-Proliferative Activities of Quinoxaline Derivatives on the K562 and MCF-7 Cell Lines. *Chemistry Research Journal* 2018, 3, 20-33.

[62]. Kpotin, G.; Gómez-Jeria, J. S. A Quantum-chemical Study of the Relationships Between Electronic Structure and Anti-proliferative Activity of Quinoxaline Derivatives on the HeLa Cell Line. *International Journal of Computational and Theoretical Chemistry* 2017, 5, 59-68.

[63]. Frisch, M. J.; Trucks, G. W.; Schlegel, H. B.; Scuseria, G. E.; Robb, M. A.; Cheeseman, J. R.; Montgomery, J., J.A.; Vreven, T.; Kudin, K. N.; Burant, J. C.; Millam, J. M.; Iyengar, S. S.; Tomasi, J.; Barone, V.; Mennucci, B.; Cossi, M.; Scalmani, G.; Rega, N. *G03 Rev. E.01*, Gaussian: Pittsburgh, PA, USA, 2007.

[64]. Gómez-Jeria, J. S. *D-Cent-QSAR: A program to generate Local Atomic Reactivity Indices from Gaussian 03 log files. v. 1.0*, v. 1.0; Santiago, Chile, 2014.

[65]. Gómez-Jeria, J. S. An empirical way to correct some drawbacks of Mulliken Population Analysis (Erratum in: J. Chil. Chem. Soc., 55, 4, IX, 2010). *Journal of the Chilean Chemical Society* 2009, 54, 482-485.

[66]. Statsoft. *Statistica v. 8.0*, 2300 East 14 th St. Tulsa, OK 74104, USA, 1984-2007.

[67]. Gómez-Jeria, J. S.; Kpotin, G. Some Remarks on The Interpretation of The Local Atomic Reactivity Indices Within the Klopman-Peradejordi-Gómez (KPG) Method. I. Theoretical Analysis. *Research Journal of Pharmaceutical, Biological and Chemical Sciences* 2018, 9, 550-561.